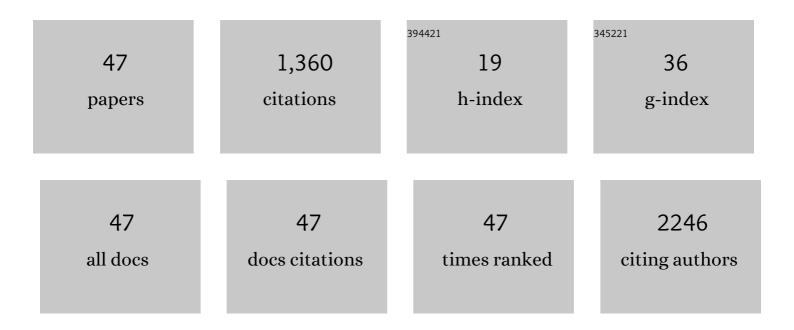
## Feng Yang

List of Publications by Year in descending order

Source: https://exaly.com/author-pdf/78713/publications.pdf Version: 2024-02-01



FENC VANG

#	Article	IF	CITATIONS
1	LncRNA CCAT1 Upregulates ATG5 to Enhance Autophagy and Promote Gastric Cancer Development by Absorbing miR-140-3p. Digestive Diseases and Sciences, 2022, 67, 3725-3741.	2.3	17
2	Lysosomal activable Vorinostat carrier-prodrug self-assembling with BPQDs enables photothermal oncotherapy to reverse tumor thermotolerance and metastasis. International Journal of Pharmaceutics, 2022, 617, 121580.	5.2	2
3	A pH-responsive complex based on supramolecular organic framework for drug-resistant breast cancer therapy. Drug Delivery, 2022, 29, 1-9.	5.7	14
4	A pH-responsive complex based on supramolecular organic framework for drug-resistant breast cancer therapy. Drug Delivery, 2022, 29, 128-137.	5.7	7
5	Chidamide stacked in magnetic polypyrrole nano-composites counter thermotolerance and metastasis for visualized cancer photothermal therapy. Drug Delivery, 2022, 29, 1312-1325.	5.7	3
6	Microneedle-based two-step transdermal delivery of Langerhans cell-targeting immunoliposomes induces a Th1-biased immune response. European Journal of Pharmaceutics and Biopharmaceutics, 2022, 177, 68-80.	4.3	6
7	Coupling Chlorin-Based Photosensitizers and Histone Deacetylase Inhibitors for Photodynamic Chemotherapy. Molecular Pharmaceutics, 2022, 19, 2807-2817.	4.6	1
8	Crystallography-guided discovery of carbazole-based retinoic acid-related orphan receptor gamma-t (RORγt) modulators: insights into different protein behaviors with "short―and "long―inverse agonists. Acta Pharmacologica Sinica, 2021, 42, 1524-1534.	6.1	5
9	Discovery of a novel 53BP1 inhibitor through AlphaScreen-based high-throughput screening. Bioorganic and Medicinal Chemistry, 2021, 34, 116054.	3.0	7
10	A Photosensitive Polymeric Carrier with a Renewable Singlet Oxygen Reservoir Regulated by Two NIR Beams for Enhanced Antitumor Phototherapy. Small, 2021, 17, e2101180.	10.0	21
11	α-Hemolysin-Aided Oligomerization of the Spike Protein RBD Resulted in Improved Immunogenicity and Neutralization Against SARS-CoV-2 Variants. Frontiers in Immunology, 2021, 12, 757691.	4.8	2
12	Polymerized vorinostat mediated photodynamic therapy using lysosomal spatiotemporal synchronized drug release complex. Colloids and Surfaces B: Biointerfaces, 2021, 205, 111903.	5.0	5
13	A Sequential Therapeutic Hydrogel With Injectability and Antibacterial Activity for Deep Burn Wounds' Cleaning and Healing. Frontiers in Bioengineering and Biotechnology, 2021, 9, 794769.	4.1	5
14	Gelated Vorinostat with inner-lysosome triggered release for tumor-targeting chemotherapy. Colloids and Surfaces B: Biointerfaces, 2020, 194, 111144.	5.0	4
15	Oligomerization of IC43 resulted in improved immunogenicity and protective efficacy against Pseudomonas aeruginosa lung infection. International Journal of Biological Macromolecules, 2020, 159, 174-182.	7.5	7
16	Rapid and Broad Immune Efficacy of a Recombinant Five-Antigen Vaccine against Staphylococcus aureus Infection in Animal Models. Vaccines, 2020, 8, 134.	4.4	32
17	YKL-40 mediates airway remodeling in asthma via activating FAK and MAPK signaling pathway. Cell Cycle, 2020, 19, 1378-1390.	2.6	15
18	Cytotoxicity induced by new spiral mesoporous silica nanorods <i>via</i> specific surface area and ROS accumulation in HeLa cells. Materials Advances, 2020, 1, 3556-3564.	5.4	3

Feng Yang

#	Article	IF	CITATIONS
19	DNA vaccine encoding OmpA and Pal from Acinetobacter baumannii efficiently protects mice against pulmonary infection. Molecular Biology Reports, 2019, 46, 5397-5408.	2.3	35
20	<p>Folate-mediated and pH-responsive chidamide-bound micelles encapsulating photosensitizers for tumor-targeting photodynamic therapy</p> . International Journal of Nanomedicine, 2019, Volume 14, 5527-5540.	6.7	24
21	<p>Magnetic And pH Dual-Responsive Nanoparticles For Synergistic Drug-Resistant Breast Cancer Chemo/Photodynamic Therapy</p> . International Journal of Nanomedicine, 2019, Volume 14, 7665-7679.	6.7	26
22	Prophylactic and therapeutic protection of human IgG purified from sera containing anti-exotoxin A titers against pneumonia caused by <i>Pseudomonas aeruginosa</i> . Human Vaccines and Immunotherapeutics, 2019, 15, 2993-3002.	3.3	2
23	Discovery of betulinaldehyde as a natural RORγt agonist. Fìtoterapìâ, 2019, 137, 104200.	2.2	7
24	Targeted eradication of gastric cancer stem cells by CD44 targeting USP22 small interfering RNA-loaded nanoliposomes. Future Oncology, 2019, 15, 281-295.	2.4	9
25	Immunization with Pseudomonas aeruginosa outer membrane vesicles stimulates protective immunity in mice. Vaccine, 2018, 36, 1047-1054.	3.8	59
26	SATB1 siRNA-encapsulated immunoliposomes conjugated with CD44 antibodies target and eliminate gastric cancer-initiating cells. OncoTargets and Therapy, 2018, Volume 11, 6811-6825.	2.0	20
27	Immunotoxicity assessment of ordered mesoporous carbon nanoparticles modified with PVP/PEG. Colloids and Surfaces B: Biointerfaces, 2018, 171, 485-493.	5.0	18
28	Structure and biological properties of mixed-ligand Cu(II) Schiff base complexes as potential anticancer agents. European Journal of Medicinal Chemistry, 2017, 134, 207-217.	5.5	90
29	Hydrophilic interaction and reversedâ€phase ultraâ€performance liquid chromatography TOFâ€MS for metabolomic analysis of <scp><i>Veratrum nigrum</i></scp> â€induced cardiotoxicity. Biomedical Chromatography, 2017, 31, e4011.	1.7	3
30	Vaccination with a recombinant OprL fragment induces a Th17 response and confers serotype-independent protection against Pseudomonas aeruginosa infection in mice. Clinical Immunology, 2017, 183, 354-363.	3.2	27
31	Activation of Endocannabinoid Receptor 2 as a Mechanism of Propofol Pretreatment-Induced Cardioprotection against Ischemia-Reperfusion Injury in Rats. Oxidative Medicine and Cellular Longevity, 2017, 2017, 1-18.	4.0	28
32	Hydrophilic mesoporous carbon nanospheres with high drug-loading efficiency for doxorubicin delivery and cancer therapy. International Journal of Nanomedicine, 2016, 11, 1793.	6.7	20
33	αâ^'Nâ^'heterocyclic thiosemicarbazone Fe(III) complex: Characterization of its antitumor activity and identification of anticancer mechanism. European Journal of Medicinal Chemistry, 2016, 123, 354-364.	5.5	67
34	Developing Anticancer Ferric Prodrugs Based on the N-Donor Residues of Human Serum Albumin Carrier IIA Subdomain. Journal of Medicinal Chemistry, 2016, 59, 7497-7511.	6.4	63
35	EPAC activation inhibits acetaldehyde-induced activation and proliferation of hepatic stellate cell via Rap1. Canadian Journal of Physiology and Pharmacology, 2016, 94, 498-507.	1.4	25
36	Protective Efficacy and Mechanism of Passive Immunization with Polyclonal Antibodies in a Sepsis Model of Staphylococcus aureus Infection. Scientific Reports, 2015, 5, 15553.	3.3	21

Feng Yang

#	Article	IF	CITATIONS
37	Effect of acid-sensing ion channel 1a on the process of liver fibrosis under hyperglycemia. Biochemical and Biophysical Research Communications, 2015, 468, 758-765.	2.1	11
38	Involvement of cAMP-PKA pathway in adenosine A1 and A2A receptor-mediated regulation of acetaldehyde-induced activation of HSCs. Biochimie, 2015, 115, 59-70.	2.6	35
39	Caffeine protects against alcohol-induced liver fibrosis by dampening the cAMP/PKA/CREB pathway in rat hepatic stellate cells. International Immunopharmacology, 2015, 25, 340-352.	3.8	76
40	Crystal structures of (1,4,7,10-tetraazacyclododecane-κ4N)bis(tricyanomethanido-κN)nickel and (1,4,7,10-tetraazacyclododecane-κ4N)(tricyanomethanido-κN)copper tricyanomethanide. Acta Crystallographica Section E: Crystallographic Communications, 2015, 71, 693-697.	0.5	0
41	Immunization with Heat Shock Protein A and $\hat{I}^3$ -Glutamyl Transpeptidase Induces Reduction on the Helicobacter pylori Colonization in Mice. PLoS ONE, 2015, 10, e0130391.	2.5	16
42	Caffeine Inhibits the Activation of Hepatic Stellate Cells Induced by Acetaldehyde via Adenosine A2A Receptor Mediated by the cAMP/PKA/SRC/ERK1/2/P38 MAPK Signal Pathway. PLoS ONE, 2014, 9, e92482.	2.5	58
43	Upâ€regulated long nonâ€coding RNA H19 contributes to proliferation of gastric cancer cells. FEBS Journal, 2012, 279, 3159-3165.	4.7	402
44	Synthesis, Structure and Magnetic Properties of Two Cobalt(II) Dicyanamide (dca) Complexes with Heterocyclic Nitrogen Donors Tetra(2â€pyridyl)pyrazine (tppz) and 2,4,6â€Tri(2â€pyridyl)â€1,3,5â€triazine (tptz) [Co <sub>2</sub> (tppz)(dca) <sub>4</sub> ]·CH <sub>3</sub> CN and [Co(tptz)(dca)(H <sub>2</sub> O)](dca). Chinese Journal of Chemistry, 2012, 30, 522-528.	<sup>:</sup> 4.9	19
45	High-Frequency Genetic Contents Variations in Clinical Candida albicans Isolates. Biological and Pharmaceutical Bulletin, 2011, 34, 624-631.	1.4	9
46	Synthesis and Characterization of Cobalt(II) and Copper(II) Tricyanomethanide (tcm) Complexes with 2,2′â€Ðipyridyl <i>N</i> , <i>N</i> ′â€Ðioxide (dpdo) as Coâ€kigands:[Co(dpdo)(tcm) <sub>2</sub> ], [Cu(dpdo)(tcm) <sub>2</sub> ] and Cu(dpdo) <sub>2</sub> (tcm) <sub>2</sub> . Chinese Journal of Chemistry, 2011, 29, 905-912.	4.9	3
47	LCâ€MS/MS method for the determination of melamine in rat plasma: Toxicokinetic study in Sprague–Dawley rats. Journal of Separation Science, 2009, 32, 2974-2978.	2.5	31